Cold Regions Science and Technology 218 (2024) 104089

Contents lists available at ScienceDirect

Cold Regions Science and Technology

journal homepage: www.elsevier.com/locate/coldregions

Solidifying saline-alkali soil with inorganic materials in a region of seasonal frost: Experiment and evaluation

Kezheng Chen [a], Lin Ding [a,b,*], Shuai Huang [c], Runqi Guo [b], Yanjie Liu [b]

[a] College of Mechanical and Electrical Engineering, Northeast Forestry University, Harbin 150040, China
[b] School of Civil Engineering, Heilongjiang University, Harbin 150080, China
[c] School of Forestry, Northeast Forestry University, Harbin 150040, China

ARTICLE INFO

Keywords:
Regions of seasonal frost
Solidified saline-alkali soil
Inorganic material
CRITIC-VIKOR model

ABSTRACT

Nine solidification approaches utilizing two inorganic materials were employed to mitigate the adverse impact of saline-alkali soil on engineering foundations and address the damage caused by freeze-thaw cycles in the Songnen Plain. The impact of inorganic material content on the shear strength of saline-alkali soil and its resistance to freeze-thaw cycles was examined. Additionally, the effectiveness of the solidification scheme was assessed concisely using the Criteria Importance Though Intercrieria Correlation - VlseKriterijumska Optimizcija I Kaompromisno Resenje (CRITIC-VIKOR) model. The findings demonstrate that both lime and fly ash enhance the shear strength of saline-alkali soil, with lime exhibiting superior effectiveness compared to fly ash. Lime induces strain-softening in the stress-strain curve of the soil. At the same time, fly ash significantly improves its resistance to freeze-thaw damage. The combined addition of lime and fly ash strikes an optimal balance between shear strength and freeze-thaw resistance. Considering mechanical performance, freeze-thaw resistance, and economic factors, scheme VII (12% lime content and 0% fly ash content) was selected based on the CRITIC-VIKOR model as the foundation for solidifying saline-alkali soil in regions of seasonal frost action.

1. Introduction

Salinization in the Songnen Plain is influenced by multiple factors, including climate, topography, geology, and hydrology. According to Bian et al. (2008) and Wang et al. (2009), the area of saline soil has exceeded 3.2×10^4 km^2. The main cations and anions in saline soil are Na^+ and HCO_3^-, respectively, with a pH of above 7.5, indicating an alkaline or strongly alkaline natural state (Bai et al., 2016; Kong et al., 2022; Yang et al., 2015). This type of soil is known as saline-alkali soil, which becomes hard when dry and has poor stability and drainage when waterlogged (Zhang et al., 2008). As a result, roads in heavily salinized areas can become seriously damaged. In addition, the collapsibility of saline-alkali soil affect the stability of channel slopes and ditches and restricts the operation of water conservancy projects (Al-Amoudi and Abduljauwad, 1995).

The Songnen Plain is located in the seasonal frost region, with the soil undergoing at least one freeze-thaw cycle yearly (Liu et al., 2010). Even daily freeze-thaw cycles occur in the surface soil in spring and autumn. These cycles weaken the mechanical properties of saline-alkali soil (Han et al., 2018). Furthermore, saline-alkali soil in the seasonally frozen ground region also exhibits significant frost heave due to the influence of temperature, salt content, moisture content, and degree of compaction, which can cause severe damage to buildings and bridges (Sun et al., 2016).

In engineering, the treatment of saline soil commonly involves replacement or solidification. Finding suitable fill materials, transportation, and storage space for saline soil requires significant human power and funds. Consequently, solidification is preferred over replacement. The solidification of saline soil can be achieved through physical, chemical, biological, or comprehensive methods (Li et al., 2014; Wang et al., 2018; Xu et al., 2020). Lime, rich in CaO, is widely used as a solidifying agent due to its ability to enhance soil strength and improve shear strength, as well as the dynamic properties of clayey soil (Consoli et al., 2014; Dash and Hussain, 2015; Fahoum et al., 1996; Gidday and Mittal, 2020; Liu et al., 2019; Poncelet and Francois, 2022; Stoltz et al., 2012; Tonini De Araújo et al., 2021; Zhang et al., 2015). Alternatively, fly ash, a byproduct of coal combustion, is often used as a partial substitute for concrete binder materials and can increase soil strength and freeze-thaw resistance (Kara De Maeijer et al., 2020; Nochaiya et al., 2010; Sharma et al., 2012; Wei et al., 2015; Yang et al.,

* Corresponding author at: College of Mechanical and Electrical Engineering, Northeast Forestry University, Harbin 150040, China.
E-mail address: 18646387888@163.com (L. Ding).

https://doi.org/10.1016/j.coldregions.2023.104089
Received 10 June 2023; Received in revised form 11 November 2023; Accepted 8 December 2023
Available online 14 December 2023

2012). Therefore, a lime and fly ash combination is proposed for solidifying saline-alkali soil on the Songnen Plain.

Prior research has introduced multiple inorganic material stabilization strategies for saline soils. Researchers frequently assess these schemes primarily based on mechanical properties and freeze-thaw resistance, often neglecting economic factors even though the cost of stabilizing saline soils is most often dictated by the practicality of implementing these schemes in engineering projects (Ding et al., 2022; Shu et al., 2023; Xia et al., 2023). Consequently, this study considered economic factors in evaluating the saline soil stabilization schemes.

In the assessment and selection of the optimal solution, various approaches are commonly used, including the Analytic Hierarchy Process (AHP), Fuzzy Comprehensive Evaluation (FCE), and VlseKriterijumska Optimizcija I Kaompromisno Resenje (VIKOR) (Opricovic, 1998; Saaty, 1987; Zadeh, 1965). The AHP is concise and practical but incorporates multiple qualitative components, diminishing its persuasiveness. Further, the FCE enables the quantitative evaluation of fuzzy data, encompassing informational content; however, its computational process is intricate, and subjectivity is pronounced. On the other hand, using VIKOR achieves a balance between maximizing group utility and minimizing individual regret to rank a limited range of decision alternatives, showcasing remarkable adaptability in assessing solution merits.

In assigning weights to the factors within each solution, objective weighting methods, such as the Coefficient of Variation, Entropy Weighting, and Criteria Importance Though Intercrieria Correlation (CRITIC), are frequently employed (Chen, 2020; Diakoulaki et al., 1995; Lotfi et al., 2010). The CRITIC comprehensively determines the objective weights of the indicators based on the comparative intensities and conflicts among evaluation criteria. Compared to other weighting methods, the CRITIC proves more suitable for this study. Consequently, the CRITIC-VIKOR model was adopted in this study to evaluate solutions for solidifying saline-alkali soil in regions characterized by seasonal freezing (Amin et al., 2022; Li et al., 2022).

This study centers on solidifying saline-alkali soil on the Songnen Plain using lime and fly ash as inorganic materials. Nine schemes were devised, and the solidified soil's shear strength and freeze-thaw resistance were examined *via* freeze-thaw cycle and triaxial tests. Subsequently, the CRITIC-VIKOR model was employed to assess and determine the optimal solidification scheme.

2. Materials and methods

2.1. Materials

2.1.1. Soil

The study focuses on representative saline-alkali soil in the Dorbet region of the Songnen Plain. To mitigate experimental errors arising from non-uniform carbonate distribution, soil samples collected from the field were desalinated and reconstituted to maintain a consistent salt content. The fundamental physical characteristics of the desalinated saline-alkali soil are presented in Fig. 1.

2.1.2. Inorganic materials

Lime (L) and fly ash (FA) were employed as inorganic solidifying agents. Lime primarily comprises CaO, whereas fly ash predominantly consists of SiO_2 and Al_2O_3. The chemical compositions of lime and fly ash are depicted in Fig. 2.

2.2. Methods

2.2.1. Solidification scheme

Based on the results of the moisture-density test, specimens were prepared with a gravimetric moisture content of 15.00% and a dry density of 1.84 g/cm^3. The compaction degree achieved 95%. Considering the carbonate content in the soda-type saline soil of the study area, the salt content in the saline-alkali soil was adjusted to 1.5%. The solidification schemes are outlined in Table 1.

2.2.2. Specimen preparation

After drying the soil, the quantified inorganic solidification materials and sodium bicarbonate were thoroughly blended. Distilled water was

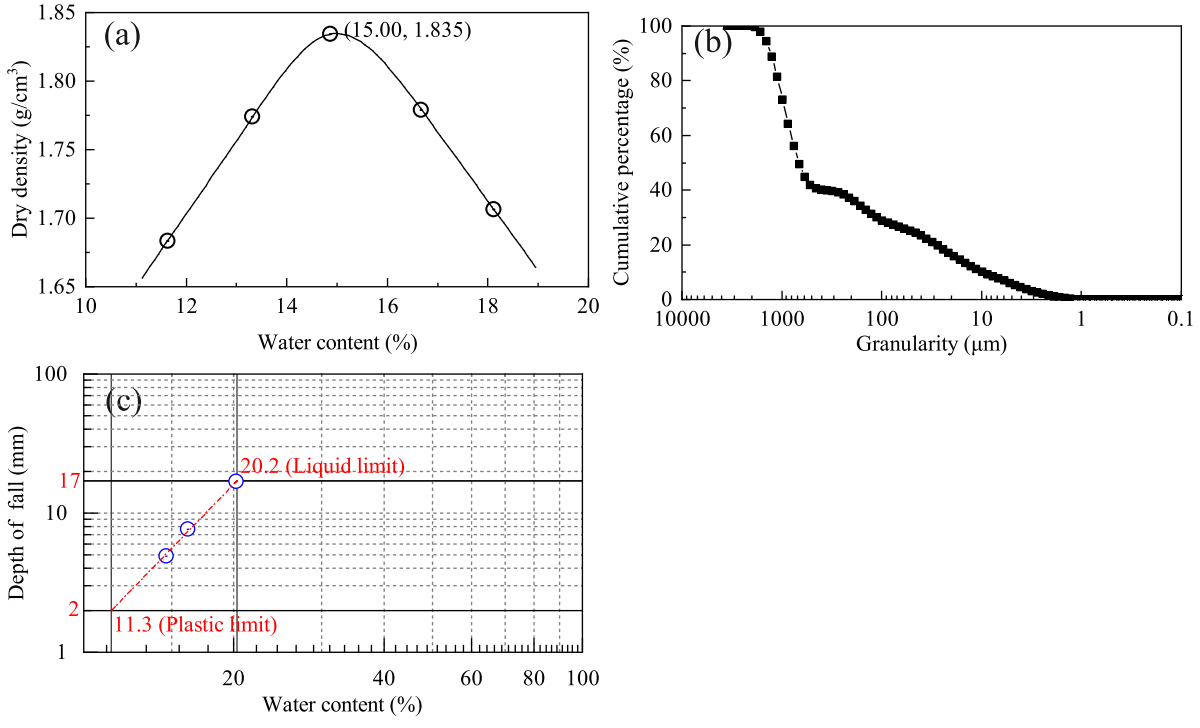

Fig. 1. Physical properties of saline-alkali soils after desalinization.
Notes: (a) moisture-density curve, (b) grain-size distribution curve, and (c) liquid limit and plastic limit.

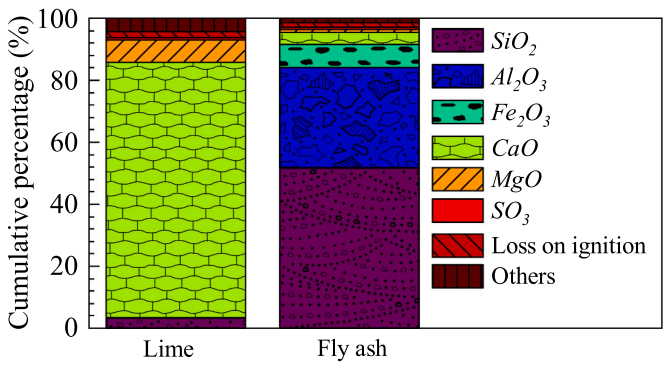

Fig. 2. Chemical composition of lime and fly ash.

gradually added to the mixture while continuously stirring, ensuring an even distribution of soil water. The prepared soil sample was subsequently sealed and allowed to rest for 24 h, enabling the water to permeate throughout the soil uniformly. Once the water distribution reached a homogeneous state, the compaction method was employed to form triaxial specimens (φ39.1 × 80 mm). It should be noted that the reaction between fly ash, lime, and water may generate hydration heat, potentially compromising the soil's structural integrity and consequently reducing its strength. To mitigate the adverse effects of hydration heat, the prepared soil samples were subjected to a 28-day curing period in an environment maintained at an air temperature of 25 °C and 95% air humidity. Following the curing period, the soil samples were subjected to 0 and 60 cycles of freeze-thaw treatment while accounting for local climatic conditions and the attenuation effect of ground temperature fluctuations with depth in the Dorbet. Each freeze-thaw cycle lasted 24 h, involving a freezing period at −25 °C for 12 h followed by thawing at 25 °C and 95% humidity for 12 h. The freeze-thaw tests were conducted using a freezer and a curing chamber for soil thawing.

2.2.3. Testing program

The tests were performed using the DYNTTS servo-controlled triaxial testing system developed by GDS, U.K. The soil samples underwent unconsolidated-undrained triaxial tests (UU) under 100, 200, and 300 kPa confining pressures. In addition, the shear rate was set at 0.8 mm/min, and the test concluded upon reaching an axial strain of 20%.

2.2.4. Data processing

The peak shear strength was determined as the shear strength at a strain of 15% for strain-hardening behavior and the maximum shear strength for strain-softening behavior. Three peak shear strengths were obtained by conducting tests at three confining pressures: 100, 200, and 300 kPa. These values were used to construct the strength and failure envelopes, allowing for the determination of the soil's cohesion (c) and internal friction angle (φ) based on the relationship between the two envelopes (Chen et al., 2022).

2.3. CRITIC-VIKOR model

The VIKOR is a compromise ranking method that seeks to attain an optimal solution by maximizing group utility and minimizing disadvantageous values when ranking finite decision alternatives (Mardani et al., 2016). The specific methodology is outlined below:

(1) Select appropriate indicators to construct the evaluation index system for the assessment objects in the study.
(2) Assess m different methods using n evaluation criteria and construct the initial decision matrix $\boldsymbol{A} = (a_{ij})_{m\times n}$, $(i = 1, 2, \ldots, m; j = 1, 2, \ldots, n)$.
(3) To remove the impact of varying dimensions on the evaluation outcomes, it is essential to normalize each index. Hence, the initial decision matrix $\boldsymbol{A}$ requires normalization, forming the standardized matrix $\boldsymbol{B} = (b_{ij})_{m\times n}$, $(i = 1, 2, \ldots, m; j = 1, 2, \ldots, n)$.

For positive indexes:

$$b_{ij} = \frac{a_{ij} - mina_j}{maxa_j - mina_j} \tag{1}$$

For negative indexes:

$$b_{ij} = \frac{maxa_j - a_{ij}}{maxa_j - mina_j} \tag{2}$$

(4) The CRITIC derives the information content of indicators by analyzing their variability and conflicts, and subsequently determines their weights according to the information content of each index.

In the CRITIC, the standard deviation is utilized to represent the variability of indices:

$$\sigma_j = \sqrt{\frac{\sum_{i=1}^{m}\left(b_{ij} - \overline{b_j}\right)^2}{m-1}} \tag{3}$$

The conflicts measure reflects the correlation among different indices, with a smaller value indicating a significant positive correlation:

$$f_j = \sum_{k=1}^{n}\left(1 - r_{jk}\right) \tag{4}$$

The r_{jk} represents the correlation between the indexes:

$$r_{jk} = \frac{\sum_{i=1}^{m}\left(b_{ij} - \overline{b_j}\right)\left(b_{ik} - \overline{b_k}\right)}{\sqrt{\sum_{i=1}^{m}\left(b_{ij} - \overline{b_j}\right)^2}\sqrt{\sum_{i=1}^{m}\left(b_{ik} - \overline{b_k}\right)^2}}, i = 1, 2, \cdots, m; j = 1, 2, \cdots, n; k = 1, 2, \cdots, n \tag{5}$$

The information content is determined by the multiplication of its variability and conflicts:

$$c_j = \sigma_j f_j \tag{6}$$

The weights of each index are expressed by the proportion of its information content in the total information content:

$$\omega_j = \frac{c_j}{\sum_{j=1}^{n} c_j} \tag{7}$$

(5) Group benefit and disadvantage values are calculated using positive and negative ideal values. Then, the compromise

Table 1
Program of solidifying saline-alkali soils with inorganic material.

Scheme	I	II	III	IV	V	VI	VII	VIII	IX
Lime	0	0	0	6%	6%	6%	12%	12%	12%
Fly ash	0	12%	24%	0	12%	24%	0	12%	24%

decision value is determined using the calculated group utility and disadvantage values:

$$x_i = \sum_{i=1}^{m}\left[\omega_j\left(\frac{b_j^+ - b_{ij}}{b_j^+ - b_j^-}\right)\right] \tag{8}$$

$$y_i = \max_{1\le j\le n}\left[\omega_j\left(\frac{b_j^+ - b_{ij}}{b_j^+ - b_j^-}\right)\right] \tag{9}$$

$$z_i = \rho\frac{x_i - x^-}{x^+ - x^-} + (1-\rho)\frac{y_i - y^-}{y^+ - y^-} \tag{10}$$

where x_i is the group benefit value; y_i is the disadvantage value; z_i is compromise decision value; b_j^+ is the positive ideal value of each index in the normalized matrix $\boldsymbol{B}$; b_j^- is the negative ideal value of each index in the normalized matrix $\boldsymbol{B}$; $x^+ = \max_{1\le i\le m} x_i$; $x^- = \min_{1\le i\le m} x_i$; $y^+ = \max_{1\le i\le m} y_i$; $y^- = \min_{1\le i\le m} y_i$; and ρ is the decision mechanism coefficient, with a value range of [0,1].

If the decision aims to maximize the collective effect, ρ should be greater than 0.5. If the decision aims to minimize the collective effect, ρ should be less than 0.5. Given that the study area is situated in a region with seasonally frost, it is crucial to consider both the mechanical properties of solidified soil (maximization of collective effect) and its resistance to freeze-thaw cycles (minimization of collective effect), while also taking into account economic considerations (minimization of collective effect). Therefore, ρ is set at 0.5 in this study.

(6) The VIKOR model determines each scheme's group benefit, disadvantage, and compromise decision value. The solidification schemes are then ranked in descending order based on these values. If the schemes meet the acceptable dominance criterion (Criterion A) and stability criterion (Criterion B), they are ranked based on the magnitude of the compromise decision value, with smaller values indicating superior schemes (Amin et al., 2022; Aminjarahi et al., 2021). In cases where Criterion B is not satisfied, z_i* and z_i** are the compromise schemes. On the other hand, if the top-ranked scheme fails to meet Criterion A but satisfies Criterion B, it is considered the overall optimal evaluation for schemes that do not meet Criterion A.

Acceptable Criterion A:

$$z_{\mathrm{i}}^{**} - z_{\mathrm{i}}^{*} \ge \frac{1}{m-1} \tag{11}$$

where z_i* is the compromise decision value of the top-ranked solution in the compromise decision value ranking; z_i^{**} is the compromise decision value of the second-ranked solution in the compromise decision value ranking, and m denotes the number of solidification schemes.

Acceptable stability Criterion B:

z_i^* corresponds to solidification scheme ranking higher than group benefit or disadvantage value.

2.4. Loss rate parameter

Additional processing is necessary to integrate diverse indices regarding the freeze-thaw resistance of inorganic solidified saline-alkali soil within the indicator layer. To accomplish this, the loss rate parameter, K, is introduced in Eq. (12):

$$K = \frac{Y_{f_0} - Y_{f_k}}{Y_{f_0}} \times 100\% \tag{12}$$

where Y_{fk} are the peak shear strength (kPa), cohesion (kPa), and internal friction angle (°) of the soil specimen after 60 freeze-thaw cycles; and Y_{f0} are the peak shear strength (kPa), cohesion (kPa), and internal friction angle (°) of the soil specimen without freeze-thaw cycles.

3. Results

3.1. Stress-strain curve

As shown in Fig. 3, the stress-strain curve of the untreated saline-alkali soil exhibits strain-hardening behavior. After solidification with fly ash, the saline-alkali soil also demonstrates strain-hardening behavior, albeit with a shorter elastic stage. In contrast, the stress-strain curves of the lime or lime-fly ash solidified saline-alkali soil exhibit strain-softening behavior. By combining the experimental results with existing literature, it is observed that the addition of inorganic materials transforms the failure mode of saline-alkali soil from plastic to brittle failures (Wang et al., 2010).

3.2. Peak shear strength

Fig. 4 shows peak shear strength. Without freeze-thaw cycles, the peak shear strength of saline-alkali soil solidified with fly ash slightly increased. On the other hand, using lime for solidification significantly enhanced peak shear strength. However, when lime is combined with fly ash, the presence of fly ash not only fails to enhance the soil's peak shear strength but also hampers the ability of lime to increase the peak shear strength of saline-alkali soil. This can be attributed to the incomplete activation of fly ash reactivity, leading to a lack of significant improvement in peak shear strength of the saline soil, as observed in the study of Zhou et al. (2022). Additionally, freeze-thaw cycles caused a reduction in the peak shear strength of the soil. However, the incorporation of fly ash can partially offset this loss.

3.3. Cohesion

Fig. 5 shows cohesion. Compared to adding lime alone or combining lime and fly ash, the improvement in cohesion of saline-alkali soil is insignificant when fly ash is added alone. Adding lime also greatly enhances the cohesion of saline-alkali soil; however, the subsequent offset of fly ash hampers the positive impact of lime on cohesion. Nevertheless, fly ash can mitigate the reduced cohesion of lime-stabilized saline-alkali soil caused by long-term freeze-thaw cycles. The significant contribution of lime to enhancing the cohesion of saline soil is well-documented in numerous studies (*e.g.*, Lyu et al., 2017; Zhou et al., 2022). Similarly, the adverse influence of fly ash on soil cohesion aligns with the findings of an analysis conducted by Cheng of factors affecting soil cohesion in regions of seasonal frost (Cheng et al., 2021).

3.4. Internal friction angle

The influence of lime and fly ash on the internal friction angle of saline soil is consistent with research by Zhou et al. (2022). As shown in Fig. 6, the sole addition of fly ash results in a slight increase in the internal friction angle of saline-alkali soil. In contrast, only adding lime leads to an approximately threefold increase in the internal friction angle. When lime is added first, followed by fly ash, the internal friction angle still experiences a minor enhancement. Freeze-thaw cycles cause a reduction in the internal friction angle of saline soil and stabilize saline soil. However, compared to peak shear strength and cohesion, the loss of the internal friction angle is negligible.

3.5. Evaluation of solidifying saline-alkali soil with inorganic materials

The following indexes were selected to evaluate the scheme of solidified saline-alkali soil: peak shear strength, cohesion, internal friction angle, rate of peak shear strength loss, rate of cohesion loss, rate of internal friction angle loss, and the cost of inorganic materials. Fig. 7 depicts this index system used to evaluate solidified saline-alkali soil

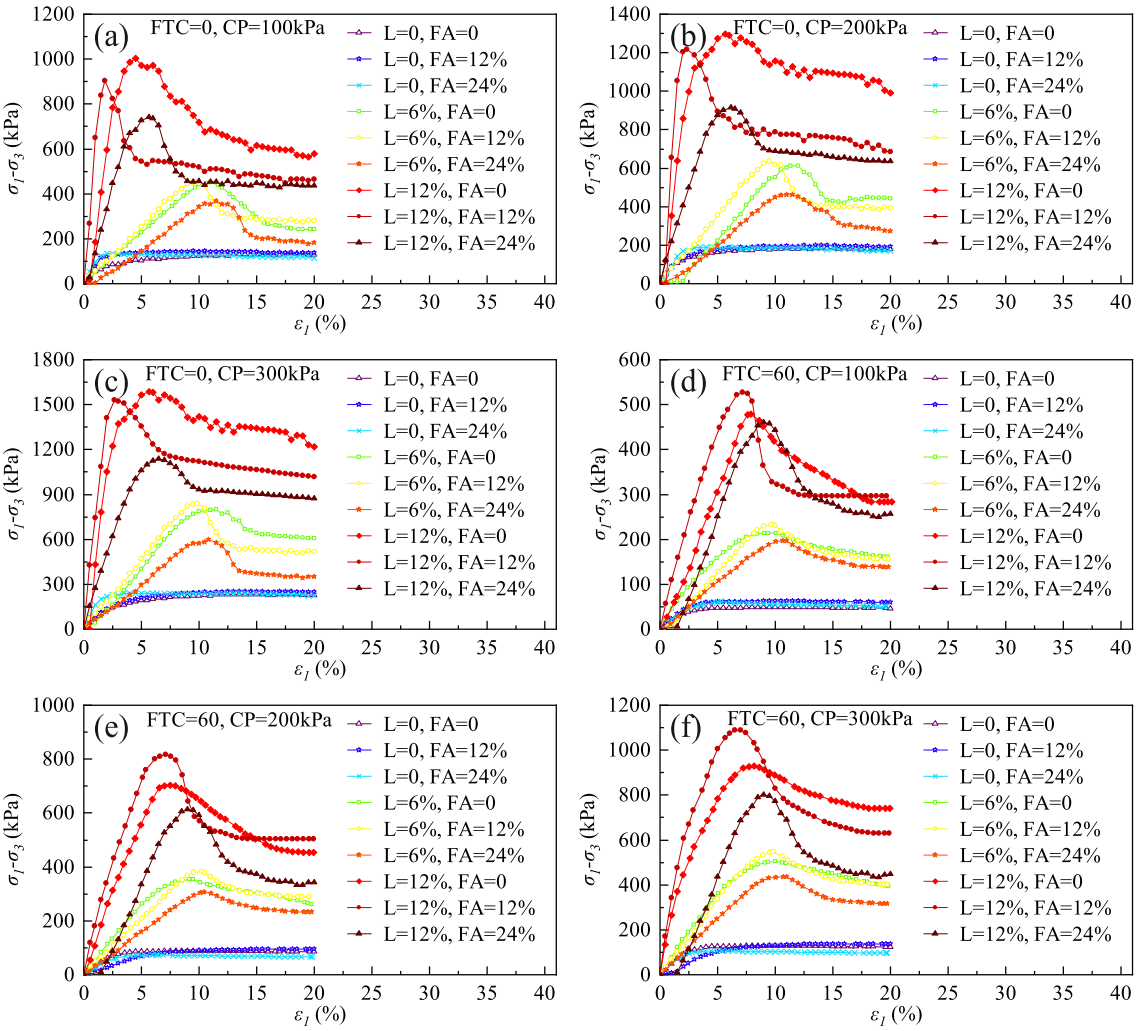

Fig. 3. Stress-strain curves of solidified saline-alkali soil.
Notes: (a) The scenario of 0 freeze-thaw cycle and 100 kPa in the confining pressure, (b) Zero freeze-thaw cycle and 200 kPa, (c) Zero freeze-thaw cycle and 300 kPa, (d) 60 freeze-thaw cycles and 100 kPa, (e) 60 freeze-thaw cycles and 200 kPa, (f) 60 freeze-thaw cycles and 300 kPa.

with inorganic materials in seasonal frost regions.

The indicator layer incorporates the peak shear strength (X_1), cohesion (X_2), and internal friction angle (X_3) as indicators of the mechanical properties of solidified inorganic saline-alkali soil (excluding freeze-thaw). These values were determined through experiments and existing or previous analyses. The peak shear strength under a confining pressure of 100 kPa was chosen as the evaluation parameter during the evaluation process. The indicators reflecting the freeze-thaw resistance of inorganic solidified saline-alkali soil were obtained using Eq. (12). The economic indicators primarily depend on the price and quantity of lime and fly ash. The lime used in the experiment was hydrated lime powder, specifically the Huigui brand, which cost 3.16 Yuan RMB/kg (URL: https://item.jd.com/65567340994.html, accessed on April 2, 2023). The fly ash used was Niedun experimental-grade Class I fly ash, priced at 7.92 Yuan RMB/kg (URL: https://item.jd.com/10034634939408.html, accessed on April 2, 2023).

Unfortunately, comparing samples directly was infeasible due to the small amount of dried soil needed per sample (167.9 g). Thus, we assumed the need to solidify 1000 kg of saline-alkali soil and employed the equal-mass substitution method to incorporate lime and fly ash into each scenario. The evaluation index values for consolidating saline-alkali soil using inorganic materials in the regions of seasonal frost can be found in Table 2.

The initial matrix $\boldsymbol{A}$ for the inorganic material solidification scheme of saline-alkali soils, obtained based on the selected index during the evaluation process, is shown in Eq. (13).

$$A = \begin{bmatrix} 131.72 & 33.65 & 11.43 & 63.79 & 90.12 & 16.40 & 0 \\ 141.53 & 34.48 & 12.55 & 56.41 & 80.35 & 15.12 & 950.40 \\ 129.85 & 31.74 & 11.85 & 53.27 & 76.37 & 14.38 & 1900.80 \\ 450.08 & 68.73 & 30.70 & 52.47 & 75.36 & 14.24 & 189.60 \\ 452.54 & 65.68 & 34.45 & 48.65 & 69.38 & 14.03 & 1140.00 \\ 367.93 & 60.52 & 27.29 & 46.57 & 65.24 & 13.96 & 2090.40 \\ 1002.75 & 179.12 & 36.45 & 52.26 & 61.05 & 11.98 & 379.20 \\ 904.74 & 145.45 & 37.62 & 41.72 & 51.96 & 8.24 & 1329.60 \\ 740.57 & 132.40 & 33.56 & 37.92 & 46.38 & 8.22 & 2280.00 \end{bmatrix} \quad (13)$$

After normalizing through Eqs. (1) and (2), the standardized matrix $\boldsymbol{B}$ is shown as Eq. (14).

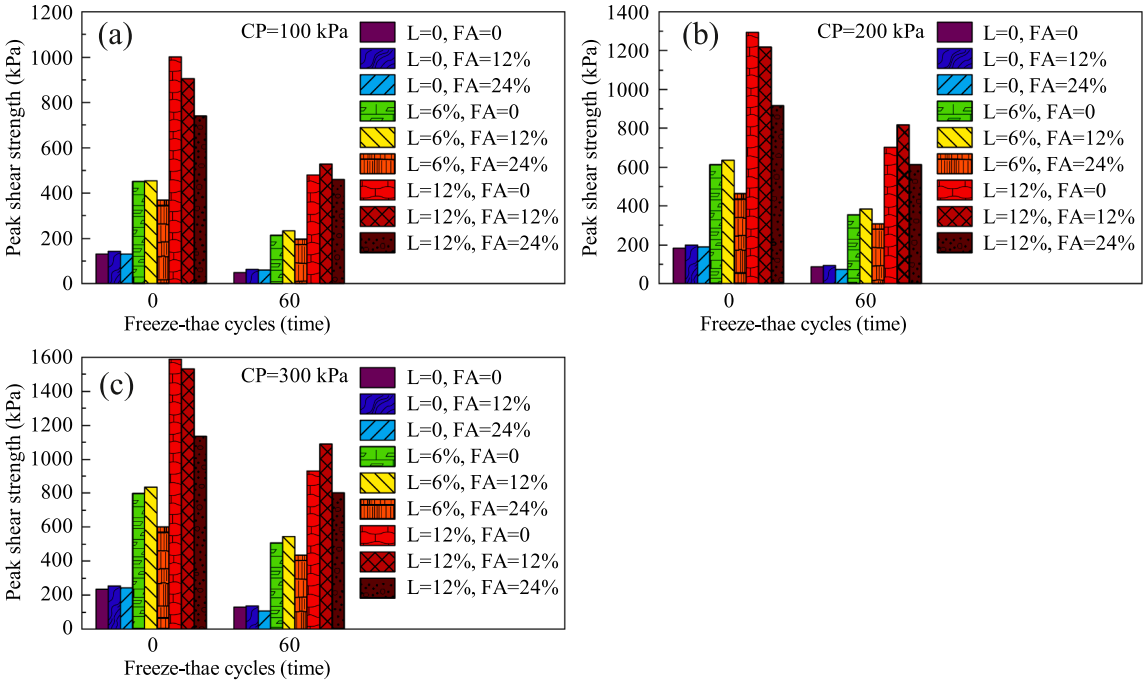

Fig. 4. Peak shear strength of solidified saline-alkali soil.
Notes: The confining pressure is (a) 100 kPa, (b) 200 kPa, and (c) 300 kPa.

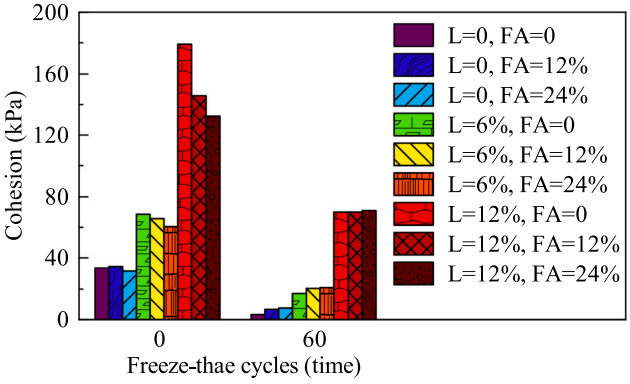

Fig. 5. Cohesion of solidified saline-alkali soil.

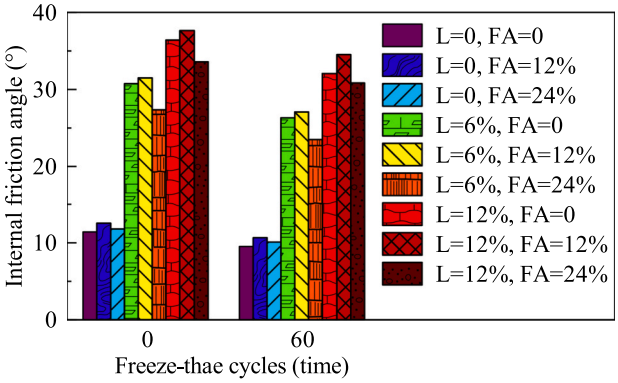

Fig. 6. Internal friction angle of solidified saline-alkali soil.

$$\boldsymbol{B} = \begin{bmatrix} 0.002 & 0.013 & 0.000 & 0.000 & 0.000 & 0.000 & 0.000 \\ 0.013 & 0.019 & 0.043 & 0.285 & 0.223 & 0.156 & 0.583 \\ 0.000 & 0.000 & 0.016 & 0.407 & 0.314 & 0.246 & 0.166 \\ 0.367 & 0.251 & 0.736 & 0.438 & 0.337 & 0.264 & 0.917 \\ 0.370 & 0.230 & 0.765 & 0.585 & 0.474 & 0.290 & 0.500 \\ 0.273 & 0.195 & 0.605 & 0.666 & 0.569 & 0.298 & 0.083 \\ 1.000 & 1.000 & 0.955 & 0.446 & 0.665 & 0.540 & 0.834 \\ 0.888 & 0.772 & 1.000 & 0.853 & 0.872 & 0.998 & 0.417 \\ 0.700 & 0.683 & 0.845 & 1.000 & 1.000 & 1.000 & 0.000 \end{bmatrix} \quad (14)$$

Table 3 presents the standard deviations of various indexes calculated using Eq. (3).

The Pearson's correlation coefficient between each index was calculated using Eq. (5). The results are shown in Fig. 8.

Next, Tables 4, 5, and 6, respectively, show the values for the conflict of each index obtained using Eq. (4), the information content of the evaluation index using Eq. (6), and the weights of each evaluation index calculated using Eq. (7).

Results depicted in Tables 7, 8, and 9 show each scheme's calculated group benefit values based on Eq. (8), disadvantage values determined using Eq. (9), and compromise decision values calculated using Eq. (10).

The solidification scheme results were subsequently arranged in ascending order based on the group benefit, disadvantage, and compromise decision values (Table 10).

Among the various schemes designed for this experiment to consider mechanical properties, freeze-thaw resistance, and economic indicators of solidifying saline-alkali soil in the regions of seasonally frozen ground, Scheme VII conforms to the CRITIC-VIKOR model's acceptable Criterion A and B. Hence, Scheme VII is considered the optimal solution.

4. Discussion

Fly ash particles exhibit features of small size and low density, enabling them to fill the voids among soil particles. This leads to

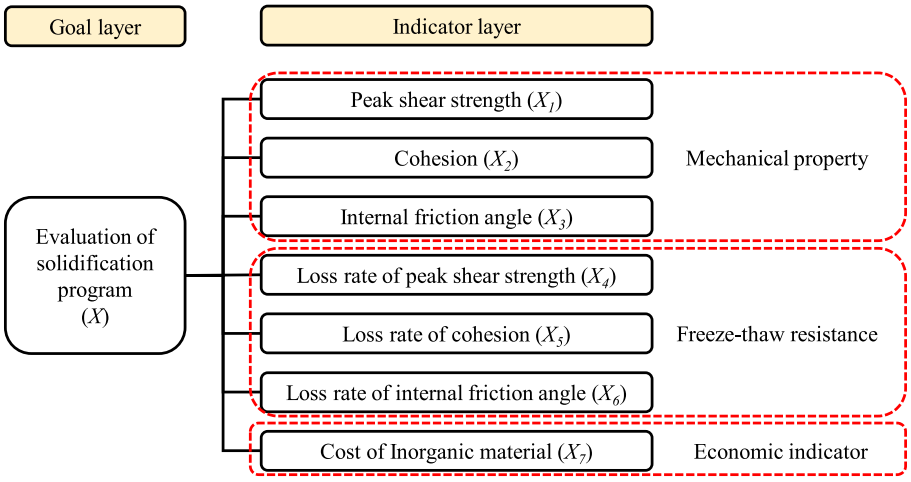

Fig. 7. Evaluation index system for solidified saline-alkali soil with inorganic materials in seasonal frost regions.

Table 2
Parameters of solidified saline-alkali soil with inorganic materials.

Schemes	Evaluation indexes						
	X_1	X_2	X_3	X_4	X_5	X_6	X_7
I	131.72	33.65	11.43	63.79	90.12	16.40	0
II	141.53	34.48	12.55	56.41	80.35	15.12	950.40
III	129.85	31.74	11.85	53.27	76.37	14.38	1900.80
IV	450.08	68.73	30.70	52.47	75.36	14.24	189.60
V	452.54	65.68	31.45	48.65	69.38	14.03	1140.00
VI	367.93	60.52	27.29	46.57	65.24	13.96	2090.40
VII	1002.75	179.12	36.45	52.26	61.05	11.98	379.20
VIII	904.74	145.45	37.62	41.72	51.96	8.24	1329.60
IX	740.57	132.40	33.56	37.92	46.38	8.22	2280.00

Table 3
Standard deviation of evaluation index.

Index	X_1	X_2	X_3	X_4	X_5	X_6	X_7
Standard deviation	0.383	0.372	0.416	0.299	0.318	0.356	0.368

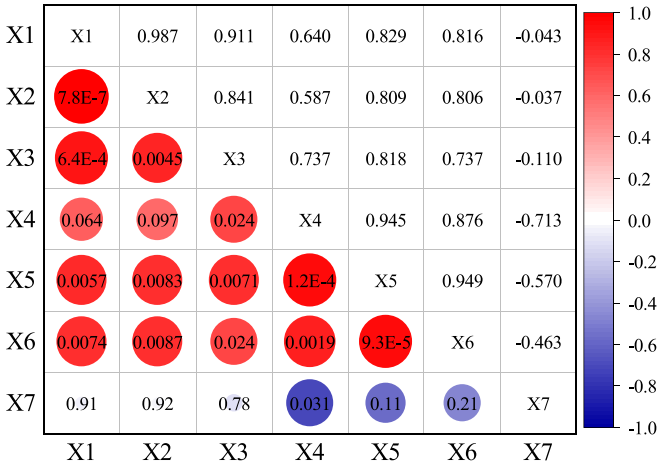

Fig. 8. Pearson's correlation coefficient between each index.
Notes: The bottom left corner represents the *p*-value, and the top right corner indicates Pearson's correlation coefficient.

Table 4
The conflict of evaluation index.

Index	X_1	X_2	X_3	X_4	X_5	X_6	X_7
Conflict	1.859	2.008	2.066	2.928	2.218	2.279	7.934

Table 5
Information content of evaluation index.

Index	X_1	X_2	X_3	X_4	X_5	X_6	X_7
Information content	0.712	0.746	0.859	0.877	0.705	0.812	2.921

Table 6
Weight of evaluation index.

Index	X_1	X_2	X_3	X_4	X_5	X_6	X_7
Weight	0.093	0.098	0.113	0.115	0.092	0.106	0.383

increased soil compaction and a slight enhancement of peak shear strength (Chen et al., 2022). Fly ash also contains Al_2O_3, Fe_2O_3, and a small amount of CaO, which react with HCO_3^- and CO_3^{2-} ions in saline-alkali soil, resulting in the production of a limited amount of binding material that improves soil cohesion (Lei et al., 2023; Lv et al., 2018). Additionally, the fine particles of fly ash contribute to uneven soil grading, thereby increasing the internal friction angle of the soil.

Conversely, lime contains a significant amount of CaO and a small quantity of MgO. These elements engage in various reactions, such as ion exchange, crystallization, volcanic ash reactions, and carbonation

Table 7
Group benefit value of each scheme.

Scheme	I	II	III	IV	V	VI	VII	VIII	IX
Group benefit value	0.616	0.699	0.833	0.398	0.524	0.695	0.212	0.285	0.459

Table 8
Individual disadvantage value of each scheme.

Scheme	I	II	III	IV	V	VI	VII	VIII	IX
Disadvantage values	0.115	0.160	0.319	0.078	0.191	0.351	0.064	0.223	0.383

Table 9
Compromise decision-making index values of each scheme.

Scheme	I	II	III	IV	V	VI	VII	VIII	IX
Compromise decision value	0.406	0.542	0.900	0.173	0.451	0.839	0.000	0.309	0.699

Table 10
Group benefit value, disadvantage value and compromise decision value of each scheme and their ranking.

Scheme	Group benefit value x_i	Disadvantage value y_i	Compromise decision value z_i	Sorting x_i	Sorting y_i	Sorting z_i
I	0.616	0.115	0.406	6	3	4
II	0.699	0.160	0.542	8	4	6
III	0.833	0.319	0.900	9	7	9
IV	0.398	0.078	0.173	3	2	2
V	0.524	0.191	0.451	5	5	5
VI	0.695	0.351	0.839	7	8	8
VII	0.212	0.064	0.000	1	1	1
VIII	0.285	0.223	0.309	2	6	3
IX	0.459	0.383	0.699	4	9	7

reactions. Some substances present in carbonate saline soil, include Na^+, K^+, H_2O, CO_2, SiO_2, and Al_2O_3 (Al-Mukhtar et al., 2010; Ouhadi and Yong, 2003). These interactions lead to the formation of new substances and novel cementitious materials, enhancing soil cohesion and structure and substantially increasing soil strength.

When both fly ash and lime are simultaneously incorporated, the cementitious materials generated by lime enhance soil cohesion and structure. However, the presence of fly ash increases soil dispersion, leading to lower cohesion and peak shear strength compared to using lime alone. Nevertheless, fly ash's fine and chemically inert particles contribute to soil heterogeneity, further elevating the internal friction angle.

In previous research concerning the stabilization of saline soils in cold regions, the primary evaluation criteria have centered on mechanical properties and freeze-thaw resistance, often overlooking the cost of stabilization (Deng et al., 2023; Qin et al., 2023; Zhou et al., 2021). Stabilization schemes for salt-affected soils that disregard cost considerations frequently encounter challenges in gaining widespread acceptance in engineering applications. In this study, the CRITIC-VIKOR model was employed to assess the stabilization schemes for saline-alkali soils. The evaluation process considered not only the mechanical properties and freeze-thaw resistance of the stabilized saline soils but also factored in the stabilization cost. From a mechanical performance perspective, Scheme VII (12% lime content and 0% fly ash content) significantly enhanced the soil's peak shear strength and cohesion. In terms of both mechanical properties and freeze-thaw resistance, Scheme VIII (12% lime content and 12% fly ash content) holds a substantial edge. When incorporating economic factors into the evaluation criteria, Scheme VII (12% lime content and 0% fly ash content) is the most suitable choice for stabilizing saline-alkali soils in cold regions.

This study devised eight inorganic material (lime and fly ash) stabilization schemes for saline-alkali soils and discussed the partial mechanical properties and freeze-thaw resistance after employing these eight schemes for soil stabilization. Furthermore, it presents the best stabilization scheme considering economic factors. However, the optimal scheme provided in this study is limited to the eight schemes we designed. In future research, additional stabilization schemes should be designed and evaluated to provide a more precise lime and fly ash content, serving as an engineering basis for stabilizing saline-alkali soils in cold regions.

5. Conclusion

(1) The stress-strain curve of saline-alkali soil shows strain-hardening behavior when fly ash is used as a single additive, albeit with reduced strain during the elastic phase. Fly ash exhibits a minor enhancement in the shear strength of saline-alkali soil but effectively mitigates long-term freeze-thaw damage.
(2) Adding lime as a single additive induces strain softening in saline-alkali soil, significantly improving its shear strength. However, its ability to mitigate long-term freeze-thaw damage is slightly inadequate.
(3) The simultaneous addition of lime and fly ash also leads to strain softening in the stress-strain curve of saline-alkali soil. Although the shear strength of the soil in this case is slightly weaker compared to that of using lime alone, it demonstrates excellent performance in mitigating long-term freeze-thaw damage.
(4) Scheme VII (12% lime content and 0% fly ash content) is the optimal solution for solidifying saline-alkali soil in regions of seasonal frost, considering their mechanical properties, freeze-thaw resistance, and economic factors. These schemes can guide engineering activities in cold regions with saline-alkali soil.

CRediT authorship contribution statement

Kezheng Chen: Methodology, Visualization, Writing – original

draft. **Lin Ding:** Conceptualization, Resources, Project administration. **Shuai Huang:** Data curation, Writing – review & editing. **Runqi Guo:** Investigation. **Yanjie Liu:** Formal analysis.

Declaration of Competing Interest

The authors declare that they have no known competing financial interests or personal relationships that could have appeared to influence the work reported in this paper.

Data availability

Data will be made available on request.

Acknowledgements

This work was funded by the Innovation Foundation for Doctoral Program of Forestry Engineering of Northeast Forestry University (No. LYGC202207), and the National Natural Science Foundation of China (No. 41071049).

References

Al-Amoudi, O.S.B., Abduljauwad, S.N., 1995. Compressibility and collapse characteristics of arid saline sabkha soils. Eng. Geol. 39, 185–202. https://doi.org/10.1016/0013-7952(95)00016-9.

Al-Mukhtar, M., Lasledj, A., Alcover, J.F., 2010. Behaviour and mineralogy changes in lime-treated expansive soil at 20°C. Appl. Clay Sci. 50, 191–198. https://doi.org/10.1016/j.clay.2010.07.023.

Amin, F., Dong, Q., Grzybowska, K., Ahmed, Z., Yan, B., 2022. A novel fuzzy-based VIKOR–CRITIC soft computing method for evaluation of sustainable supply chain risk management. Sustainability 14, 2827. https://doi.org/10.3390/su14052827.

Aminjarahi, M., Abdoli, M., Fadaee, Y., Kohan, F., Shokouhyar, S., 2021. The prioritization of lean techniques in emergency departments using VIKOR and SAW approaches. Ethiop. J. Health Sci. 31, 283–292. https://doi.org/10.4314/ejhs.v31i2.11.

Bai, L., Wang, C., Zang, S., Zhang, Y., Hao, Q., Wu, Y., 2016. Remote sensing of soil alkalinity and salinity in the Wuyu'er-Shuangyang river basin, Northeast China. Remote Sens. 8, 163. https://doi.org/10.3390/rs8020163.

Bian, J., Tang, J., Lin, N., 2008. Relationship between saline-alkali soil formation and neotectonic movement in Songnen Plain. China. Environ. Geol. 55, 1421–1429. https://doi.org/10.1007/s00254-007-1092-0.

Chen, C., 2020. A novel multi-criteria decision-making Model for building material supplier selection based on entropy-AHP weighted TOPSIS. Entropy 22, 259. https://doi.org/10.3390/e22020259.

Chen, K., Huang, S., Liu, Y., Ding, L., 2022. Improving carbonate saline soil in a seasonally frozen region using lime and fly ash. Geofluids 2022, 7472284. https://doi.org/10.1155/2022/7472284.

Cheng, Z., Cui, G., Gao, Y., Gang, H., Gao, Z., Yang, Z., Zhang, X., 2021. Mechanical properties of fly ash reinforced subgrade soil in seasonally frozen area. Bull. Chinese Ceramic Soc. 40 https://doi.org/10.16552/j.cnki.issn1001-1625.20210906.006, 3854-3864+3875.

Consoli, N.C., Prietto, P.D.M., Lopes Jr., L. da S., Winter, D., 2014. Control factors for the long term compressive strength of lime treated sandy clay soil. Transp. Geotech. 1, 129–136. https://doi.org/10.1016/j.trgeo.2014.07.005.

Dash, S.K., Hussain, M., 2015. Influence of lime on shrinkage behavior of soils. J. Mater. Civ. Eng. 27, 04015041. https://doi.org/10.1061/(ASCE)MT.1943-5533.0001301.

Deng, T., Deng, Y., Yue, X., Cui, Y., 2023. Deterioration of marine soft clay at East China solidified by cement–metakaolin composite. Environ. Geotech. 10, 57–65. https://doi.org/10.1680/jenge.18.00202.

Diakoulaki, D., Mavrotas, G., Papayannakis, L., 1995. Determining objective weights in multiple criteria problems: the critic method. Comput. Oper. Res. 22, 763–770. https://doi.org/10.1016/0305-0548(94)00059-H.

Ding, Q., Hu, Z., Huang, S., Chen, K., Liu, Y., Ding, L., 2022. An investigation of non-linear strength characteristics of solidified saline soils in cold regions. Materials 15, 7594. https://doi.org/10.3390/ma15217594.

Fahoum, K., Aggour, S., Amini, F., 1996. Dynamic properties of cohesive soils treated with lime. J. Geotech. Eng. 122, 382–389. https://doi.org/10.1061/(ASCE)0733-9410(1996)122:5(382).

Gidday, B.G., Mittal, S., 2020. Improving the characteristics of dispersive subgrade soils using lime. Heliyon 6, e03384. https://doi.org/10.1016/j.heliyon.2020.e03384.

Han, Y., Wang, Q., Wang, N., Wang, J., Zhang, X., Cheng, S., Kong, Y., 2018. Effect of freeze-thaw cycles on shear strength of saline soil. Cold Reg. Sci. Technol. 154, 42–53. https://doi.org/10.1016/j.coldregions.2018.06.002.

Kara De Maeijer, P., Craeye, B., Snellings, R., Kazemi-Kamyab, H., Loots, M., Janssens, K., Nuyts, G., 2020. Effect of ultra-fine fly ash on concrete performance and durability. Constr. Build. Mater. 263, 120493 https://doi.org/10.1016/j.conbuildmat.2020.120493.

Kong, F., Nie, L., Xu, Y., Rui, X., He, Y., Zhang, T., Wang, Y., Du, C., Bao, C., 2022. Effects of freeze-thaw cycles on the erodibility and microstructure of soda-saline loessal soil in northeastern China. Catena 209, 105812. https://doi.org/10.1016/j.catena.2021.105812.

Lei, B., Fu, P., Wang, Xiaoli, Ni, W., Zhang, S., Wang, Xiancong, Shi, J., Xu, M., 2023. The hydration mechanisms of co-stabilization saline soils by using multiple solid wastes. Processes 11, 2679. https://doi.org/10.3390/pr11092679.

Li, J., Pu, L., Han, M., Zhu, M., Zhang, R., Xiang, Y., 2014. Soil salinization research in China: advances and prospects. J. Geogr. Sci. 24, 943–960. https://doi.org/10.1007/s11442-014-1130-2.

Li, X., Han, Z., Yazdi, M., Chen, G., 2022. A CRITIC-VIKOR based robust approach to support risk management of subsea pipelines. Appl. Ocean Res. 124, 103187 https://doi.org/10.1016/j.apor.2022.103187.

Liu, J., Wang, T., Tian, Y., 2010. Experimental study of the dynamic properties of cement- and lime-modified clay soils subjected to freeze-thaw cycles. Cold Reg. Sci. Technol. 61, 29–33. https://doi.org/10.1016/j.coldregions.2010.01.002.

Liu, Y., Wang, Q., Liu, S., Shangguan, Y., Fu, H., Ma, B., Chen, H., Yuan, X., 2019. Experimental investigation of the geotechnical properties and microstructure of lime-stabilized saline soils under freeze-thaw cycling. Cold Reg. Sci. Technol. 161, 32–42. https://doi.org/10.1016/j.coldregions.2019.03.003.

Lotfi, F.H., Nematollahi, N., Behzadi, M.H., Mirbolouki, M., 2010. Ranking decision making units with stochastic data by using coefficient of variation. Math. Comput. Appl. 15, 148–155. https://doi.org/10.3390/mca15010148.

Lv, Q., Jiang, L., Ma, B., Zhao, B., Huo, Z., 2018. A study on the effect of the salt content on the solidification of sulfate saline soil solidified with an alkali-activated geopolymer. Constr. Build. Mater. 176, 68–74. https://doi.org/10.1016/j.conbuildmat.2018.05.013.

Lyu, Q., Chai, S., Li, M., 2017. An experimental study of the shear properties of the solidified saline soil with lime concerning under the influence of multiple factors. Hydrogeol. Eng. Geol. 44, 89–95. https://doi.org/10.16030/j.cnki.issn.1000-3665.2017.06.14.

Mardani, A., Zavadskas, E.K., Govindan, K., Senin, A.A., Jusoh, A., 2016. VIKOR technique: a systematic review of the state of the art literature on methodologies and applications. Sustainability 8, 37. https://doi.org/10.3390/su8010037.

Nochaiya, T., Wongkeo, W., Chaipanich, A., 2010. Utilization of fly ash with silica fume and properties of Portland cement–fly ash–silica fume concrete. Fuel 89, 768–774. https://doi.org/10.1016/j.fuel.2009.10.003.

Opricovic, S., 1998. Multicriteria Optimization of Civil Engineering Systems. Faculty of Civil Engineering, Belgrade.

Ouhadi, V.R., Yong, R.N., 2003. The role of clay fractions of marly soils on their post stabilization failure. Eng. Geol. 70, 365–375. https://doi.org/10.1016/S0013-7952(03)00104-2.

Poncelet, N., Francois, B., 2022. Effect of laboratory compaction mode, density and suction on the tensile strength of a lime-treated silty soil. Transp. Geotech. 34, 100763 https://doi.org/10.1016/j.trgeo.2022.100763.

Qin, H., Wang, Yonghui, Wang, Yanning, 2023. Mechanical properties and microscopic mechanism of active MgO-fly ash solidified saline soil in seasonal freezing areas. Constr. Build. Mater. 393, 132093 https://doi.org/10.1016/j.conbuildmat.2023.132093.

Saaty, R.W., 1987. The analytic hierarchy process—what it is and how it is used. Math. Model. 9, 161–176. https://doi.org/10.1016/0270-0255(87)90473-8.

Sharma, N.K., Swain, S.K., Sahoo, U.C., 2012. Stabilization of a clayey soil with fly ash and lime: a micro level investigation. Geotech. Geol. Eng. 30, 1197–1205. https://doi.org/10.1007/s10706-012-9532-3.

Shu, H., Yu, Q., Niu, C., Liu, J., Xia, W., Sun, X., Wang, Z., Wang, Q., 2023. Effect of dry-wet cycles on the mechanical properties of saline soil solidified with sulfur-free lignin and hydrophobic polymer. J. Build. Eng. 76, 107116 https://doi.org/10.1016/j.jobe.2023.107116.

Stoltz, G., Cuisinier, O., Masrouri, F., 2012. Multi-scale analysis of the swelling and shrinkage of a lime-treated expansive clayey soil. Appl. Clay Sci. 61, 44–51. https://doi.org/10.1016/j.clay.2012.04.001.

Sun, D., Wang, W., Wang, Q., Chen, J., Chen, C., 2016. Characteristics and prediction of frost heave of saline soil in western Jilin province. Int. J. Heat Technol. 34, 709–714. https://doi.org/10.18280/ijht.340422.

Tonini De Araújo, M., Tonatto Ferrazzo, S., Jordi Bruschi, G.J., Consoli, N.C., 2021. Mechanical and environmental performance of eggshell lime for expansive soils improvement. Transp. Geotech. 31, 100681 https://doi.org/10.1016/j.trgeo.2021.100681.

Wang, L., Seki, K., Miyazaki, T., Ishihama, Y., 2009. The causes of soil alkalinization in the Songnen Plain of Northeast China. Paddy Water Environ. 7, 259–270. https://doi.org/10.1007/s10333-009-0166-x.

Wang, P., Wang, X., Chai, S., 2010. Solidifying methods for inshore saline soil and its deviator stress-strain. Rock Soil Mech. 31, 3939–3944. https://doi.org/10.16285/j.rsm.2010.12.043.

Wang, X., Xing, X., Zhang, F., Xin, K., 2018. Biological improvement of saline alkali soil reference system: a review. Sci. Cold Arid Reg. 10, 516–521. https://doi.org/10.3724/SP.J.1226.2018.00516.

Wei, H., Jiao, Y., Liu, H., 2015. Effect of freeze–thaw cycles on mechanical property of silty clay modified by fly ash and crumb rubber. Cold Reg. Sci. Technol. 11, 70–77. https://doi.org/10.1016/j.coldregions.2015.04.004.

Xia, W., Wang, Q., Yu, Q., Yao, M., Sun, D., Liu, J., Wang, Z., 2023. Experimental investigation of the mechanical properties of hydrophobic polymer-modified soil subjected to freeze–thaw cycles. Acta Geotech. 18, 3623–3642. https://doi.org/10.1007/s11440-023-01804-9.

Xu, C., Dong, Y., Lu, J., Zhang, Y., Cheng, Mengqi, Cheng, Mengyu, Ma, J., 2020. Research progress of soil improvement and soil resources utilization of coastal

saline-alkaline land in China. World For. Res. 33, 68–73. https://doi.org/10.13348/j.cnki.sjlyyj.2020.0056.y.

Yang, X., Liu, J., Dang, J., 2012. Experimental research on the engineering property of chlorine saline soil improved by fly ash. J. Yangtze River Sci. Res. Inst. 29, 82–86. https://doi.org/10.3969/j.issn.1001-54852012.11.01.

Yang, F., Wang, Z., Wang, Y., An, F., Yang, H., 2015. Soil water characteristic of saline-sodic soil in Songnen plain. Sci. Geog. Sinica 35, 340–345. https://doi.org/10.13249/j.cnki.sgs.2015.03.012.

Zadeh, L.A., 1965. Fuzzy sets. Inf. Control. 8, 338–353. https://doi.org/10.1016/S0019-9958(65)90241-X.

Zhang, G., Li, J., Yu, Q., Zhang, B., Yang, R., Chen, H., 2008. Influence of salt content on shearing strength of the carbonate saline soil in Songnen (Songhuajiang River-Nenjiang River) Plain. Chinese J. Geol. Hazard Control 19, 128–131. https://doi.org/10.16031/j.cnki.issn.1003-8035.2008.01.031.

Zhang, X., Mavroulidou, M., Gunn, M.J., 2015. Mechanical properties and behaviour of a partially saturated lime-treated, high plasticity clay. Eng. Geol. 193, 320–336. https://doi.org/10.1016/j.enggeo.2015.05.007.

Zhou, Y., Guan, Q., Yan, P., 2021. Investigation of freeze-thaw resistance of stabilized saline soil. Adv. Civ. Eng. 2021, e5555436 https://doi.org/10.1155/2021/5555436.

Zhou, C., Cui, H., Zhang, Z., Chi, G., Chen, S., 2022. Mechanical properties of improved carbonate soil roadbed filler. J. Harbin Inst. Technol. 54, 93–100. https://doi.org/10.11918/202110111.